## General Disclaimer

## One or more of the Following Statements may affect this Document

- This document has been reproduced from the best copy furnished by the organizational source. It is being released in the interest of making available as much information as possible.

- This document may contain data, which exceeds the sheet parameters. It was furnished in this condition by the organizational source and is the best copy available.

- This document may contain tone-on-tone or color graphs, charts and/or pictures, which have been reproduced in black and white.

- This document is paginated as submitted by the original source.

- Portions of this document are not fully legible due to the historical nature of some of the material. However, it is the best reproduction available from the original submission.

Produced by the NASA Center for Aerospace Information (CASI)

**NASA TECHNICAL MEMORANDUM**

NASA TM-73857

NASA TM-73857

(NASA-TM-73857) PERFORMANCE CHARACTERISTICS OF TWO ANNULAR DUMP DIFFUSERS USING SUCTION-STABILIZED VORTEX FLOW CONTROL (NASA) 14 p HC A02/MF A01 CSCL 01A

N78-19057

Unclas
G3/02 09449

# PERFORMANCE CHARACTERISTICS OF TWO ANNULAR DUMP DIFFUSERS USING SUCTION-STABILIZED VORTEX FLOW CONTROL

by A. J. Juhasz and J. M. Smith
Lewis Research Center
Cleveland, Ohio 44135

TECHNICAL PAPER to be presented at the
Joint Symposium on Design and Operation of Fluid Machinery
cosponsored by the International Association for Hydraulic
Research, the American Society of Mechanical Engineers, and
the American Society of Civil Engineers
Fort Collins, Colorado, June 12-14, 1978

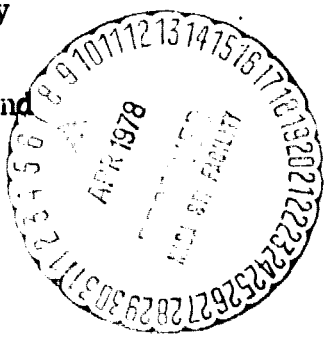

# PERFORMANCE CHARACTERISTICS OF TWO ANNULAR DUMP DIFFUSERS USING SUCTION-STABILIZED VORTEX FLOW CONTROL

A. J. Juhasz and J. M. Smith
NASA-Lewis Research Center
Cleveland, Ohio 44135

E-9011-1

## ABSTRACT

Test results are described for two abrupt area change annular diffusers with provisions for maintaining suction stabilized toroidal vortices at the area discontinuity. Both diffusers had an overall area ratio of 4.0 with the prediffuser area ratio being 1.18 for diffuser A and 1.4 for diffuser B. Performance was evaluated at near atmospheric pressure and temperature for a range of inlet Mach numbers from 0.18 to 0.41 and suction rates from 0 to 18%. Static pressure recovery improved significantly as the suction rate was increased to approximately 11%. Results obtained with diffuser A were superior to that obtained with diffuser B. Flat radial profiles of exit velocity were not obtained since the flow showed preferential hub or tip attachment at moderate suction rates. At high suction rates the diffuser exit flow became circumferentially nonuniform and unstable.

Des résultats expérimentaux sont presentés pour deux diffuseurs annulaires characterisés par un changement abrupt de la section du passage de l'air et par des tourbillons annulaires stabilisés par une aspiration de l'air à la discontinuité de la section du passage. Le rapport d'ouverture total des deux diffuseurs était égal à 4.0; le rapport d'ouverture de l'ajutage en avant de diffuseur A était égal à 1.18 et égal à 1.4 en avant de diffuseur B. Les essais de fonctionnement des diffuseurs ont étés conduits à une pression et à une température voisines d'atmospheriques. Le nombre de Mach à l'entrée était varié entre 0.18 et 0.41. L'aspiration était reglée de 0 à 18% d'écoulement total du diffuseur. Dans les deux diffuseurs la récuperation de la pression statique augmentait d'une manière significative avec l'accroissement du débit aspiré jusqu'au 11% de'écoulement total. L'efficacité du diffuseur A était supérieur à celle du diffuseur B. A des débits de l'aspiration moderés les profils de la vitesse axiale à la sortie des diffuseurs n'étaient pas plats mais biaisés vers ou la paroi interne ou la paroi externe du passage annulaire. Avec un débit de l'aspiration elevé (supérieur à 11%) l'écoulement à la sortie des diffuseurs devenait non uniforme et une instabilité apparissait.

## INTRODUCTION

The operation of an annular diffuser using suction-stabilized toroidal vortices on both inner and outer walls is analogous to that of a two-dimensional diffuser utilizing rotating cylindrical walls: the rotation of the solid boundary preferentially with the flow reduces the adverse wall pressure gradients thus permitting flow expansion to higher area ratios without flow separation. In an annular diffuser the rotating cylindrical walls are replaced by toroidal vortices formed as a result of the wall geometry design with provisions for vortex stabilization such as suction or bleed.

The use of standing vortices to control flow expansion was originally proposed by Ringleb (ref. 1) based on observations of mountain ridge vortex flows which cause snow cornice formation. Hence the Ringleb diffuser was designed with precisely contoured cusps in the diffuser walls intended for vortex trapping, but no provisions for replenishing vortex energy dissipated by friction were available. As a result this diffuser achieved only limited success.

To overcome this problem the use of suction was proposed for vortex stabilization and a number of step area change diffusers using suction stabilized vortices were tested, (refs. 2 to 7). Diffuser effectiveness values over 90% were reported in Ref. 6, obtained by using flat rings or "vortex fences" which were positioned on each wall a short distance downstream of a diffuser approach passage. The good performance was attributed to the design feature which permitted positioning the vortices inside the suction chambers, rather than downstream of them. However, tests with a similar geometry, Ref. 7, while confirming good pressure recovery at moderate suction rates, revealed a circumferential flow nonuniformity and flow instability when a total suction rate of approximately 10% was exceeded.

The purpose of this report is to present the highlights of test results, particularly or circumferential flow uniformity, obtained with two annular diffusers utilizing suction stabilized vortex flow control. Both diffusers had the same overall area ratio but different prediffuser area ratios and suction slot geometries. Velocity profile and diffuser pressure recovery performance data were obtained at ambient pressure and temperature, with inlet Mach numbers ranging from 0.18 to 0.41 and suction rate varying from zero to 18% of total inlet mass flow rate.

## SYMBOLS

| | |
|---|---|
| A | area |
| AP | prediffuser area ratio |
| AR | diffuser area ratio |
| B | bleed-flow fraction of total mass-flow rate |
| $g_c$ | dimensional constant |
| H | diffuser inlet passage height |
| L | distance from vortex fence to exit pitot static rakes |

| | |
|---|---|
| M | average Mach number at an axial station |
| $M_r$ | local Mach number at a radial position |
| m | mass-flow rate |
| P | average pressure at an axial station |
| p | local pressure at a radial position |
| R | gas constant for air |
| S | suction rate, percent |
| T | temperature |
| V | average velocity at an axial station |
| $\nu$ | local velocity at a radial position |
| X | axial gap between vortex fence and exit of prediffuser (see fig. 2) |
| Y | radial gap between vortex fence and exit (see fig. 2) |
| $\alpha$ | kinetic energy flux parameter = $\frac{1}{A}\int\left(\frac{\nu}{V}\right)^3 dA$ |
| $\gamma$ | specific-heat ratio |
| $\theta$ | prediffuser half angle |
| $\eta$ | diffuser effectiveness, eq. (3) |

Subscripts:

| | |
|---|---|
| i | inner wall |
| m | maximum |
| o | outer wall |
| r | local value at given radial position |
| t | total |
| 0 | stagnation condition |
| 1 | diffuser inlet station |
| 2 | diffuser exit station |

## APPARATUS AND INSTRUMENTATION

### Flow System

Details of the test facility are given in Ref. 4 and only a general overview is included here. Air from a remotely located compressor station is ducted at a nominal pressure of $10^6$ pascals (145 psia) and ambient temperature to the facility where it supplies the "main flow" to the test diffuser and the primary flows for two ejectors which are used to generate the vacuum required for the inner and outer wall suction flows. After being metered by a standard flange tap ASME orifice run the main flow is throttled to near atmospheric pressure as it enters a mixing chamber from which it flows through the test diffuser. The ejector secondary flows, or suction flows, are metered at subatmospheric pressure by standard ASME orifices.

## Diffuser Test Apparatus

An axial section of the apparatus is shown in Fig. 1. The component parts are assembled onto a 91 cm (36 in) mounting flange and can then be bolted as a unit onto the downstream flange of the diffuser air mixing chamber. The main parts are a centerbody with attached inner wall suction plenum with associated piping, needed to duct inner wall suction flow to an ejector, and an outer housing having a transparent lucite wall for flow observations. An outer wall suction manifold is mounted on this outer housing. The removable diffuser walls are located at the junction of inlet and exit passages.

## Diffuser Walls

Details of diffuser wall geometry and location of instrumentation common to the two diffusers tested are shown in Fig. 2. Differences between the two geometries are pointed out in Table I. For both diffusers the suction slots on both the inner and the outer wall are formed by the prediffuser trailing edge and a variable position flat metal ring referred to as a vortex fence. The radial gap between the trailing edge of the prediffuser and the outer diameter of the flat ring is shown as the Y dimension in Fig. 2. This radial gap was varied over a number of values. The axial gap, or X dimension, was also varied by successively positioning the rings at various axial positions. Optimum values of both radial gap, Y, and axial gap, X were determined for both diffusers, based on best overall performance at constant suction rate during preliminary screening tests. These values are listed in Table I which summarizes the final geometric details for each diffuser, which remained constant during the main performance tests.

TABLE I: FINAL DIFFUSER GEOMETRY

| Diffuser | Overall area ratio | Prediffuser | | Radial gap | Axial gap |
|---|---|---|---|---|---|
| | | Area ratio | Half angle | | |
| A | 4.0 | 1.15 | $3.5^{\circ}$ | 0.15 H | 0.45 H |
| B | 4.0 | 1.40 | $7.5^{\circ}$ | 0.05 H | 0.30 H |

where H is the diffuser inlet passage height.

## Diffuser Instrumentation

Essential instrumentation located in the diffuser inlet and exit planes is shown in Figs. 1 and 2. Diffuser inlet total pressure was obtained from three five-point total pressure rakes which were equally spaced around the annular circumference in the diffuser inlet plane. Inlet static pressure was measured by three equally spaced outer wall taps. Diffuser exit total and static pressures were measured by three nine-point pitot static rakes. These were mounted on a moveable bracket which maintained a fixed 120 degree spacing between the rakes but permitted them to be traversed in a circumferential direction and to be translated axially. Although data were

taken with the rakes positioned at several locations in the diffuser exit plane, results reported here are for the exit rakes located downstream of the vortex fences at a distance equal to six inlet passage heights.

A limited amount of data were also taken in the prediffuser exit plane using a traversing pitot-static probe and flow visualization tufts. All data were remotely recorded on magnetic tape for subsequent computer processing.

## PROCEDURE

### Performance Parameters

The overall performance of the diffusers was evaluated in terms of radial profile of exit velocity including circumferential uniformity, diffuser effectiveness and total pressure loss. Intermediate computations included both circumferentially and radially averaged total and static pressures, local and average Mach numbers, and local-to-average Mach number ratios used to generate velocity profile plots. Local Mach numbers were computed for each pitot-static probe position from the relation

$$M_r = \sqrt{\frac{2}{\gamma - 1}\left(\frac{P_0}{p}\right)^{\frac{\gamma-1}{\gamma}} - 1} \tag{1}$$

Radial and circumferential averages of the values computed by eq. (1) were taken to obtain average Mach numbers at the diffuser inlet and exit planes. As a check on the arithmetically averaged $M_1$ a mean effective inlet Mach number was also computed by iteration from inlet airflow rate, total pressure, temperature, and area data as they relate in the expression:

$$M_1 = \frac{\dot{m}_1}{P_{01}A_1}\sqrt{\frac{RT_{01}}{\gamma g_c}}\left(1 + \frac{\gamma - 1}{2}M_1^2\right)^{(\gamma+1)/2(\gamma-1)} \tag{2}$$

The velocity ratios at each radial position, needed to generate velocity profiles, were obtained from the circumferential averages of the local- to average-Mach-number ratios. A plotting routine was used to generate the velocity profiles by computer with output on microfilm.

Diffuser effectiveness was computed from the following relation:

$$\eta = \frac{P_2 - P_1}{(P_{01} - P_1)\left[1 - \left(\frac{1 - B}{AR}\right)^2\right]} \times 100 \tag{3}$$

The total-pressure loss was defined as

$$\frac{\Delta P_0}{P_{01}} = \frac{P_{01} - P_{02}}{P_{01}} \times 100 \tag{4}$$

## Test Conditions

Typical diffuser inlet conditions were the following:

| | |
|---|---|
| Total pressure, pascals (psia) | $9.86\times10^4$ to $10.45\times10^4$ (14.29 to 15.22) |
| Static pressure, pascals (psia) | $9.39\times10^4$ to $9.88\times10^4$ (13.62 to 14.32) |
| Temperature, K ($^{o}$F) | 277 to 289 (39 to 60) |
| Mach number | 0.18 to 0.41 |
| Velocity, m/sec (ft/sec) | 61 to 134 (199 to 450) |
| Reynolds number (based on inlet passage height) | $2.1\times10^5$ to $4.8\times10^5$ |
| Bleed rate, percent of total flow | 0 to 18.0 |

## DISCUSSION OF RESULTS

Due to space limitations, performance characteristics that were generally similar for both diffusers are presented as typical. A performance comparison is made only where significantly different results were obtained.

### Radial Profiles of Inlet Velocity

The profiles of Fig. 3 were generated by plotting the ratio of local inlet velocity at a radial position to the average inlet velocity. Profiles in three different circumferential planes, as measured by the three equally spaced inlet rakes are shown on the right side and the circumferentially averaged profile is shown on the left side of Figs. 3(a) and (b). Although diffuser effectiveness results will be discussed under a separate heading, some values for this parameter as determined from individual rake measurements are shown for each figure because they reflect variations in inlet static pressure and hence give further indication about circumferential uniformity of the inlet flow. The profiles of Fig. 3(a), obtained at a total suction rate of 9.9% (split between inner and outer wall in the ratio of 40/60), are typical for both diffusers operating at suction rates from zero to about 10%. The profiles show a mild hub bias, characteristic for flow in annular passages. The kinetic energy flux parameter, $\alpha_1$, for these profiles was less than 1.01, and it was not varied during the test program. The circumferential uniformity of the individual rake profiles is seen to be within ±4% at 9.9% suction, and diffuser effectiveness values computed from individual rake data are within 6% of each other. As suction rate is increased to 12.3% (fig. 3(b)) circumferential uniformity deteriorates to about ±10% and diffuser effectiveness values deviate from each other by over 14%. The effectiveness of the rake 2 position actually decreases with increasing suction suggesting that a separation bubble is established downstream of rake 2 which causes a decrease of inlet flow in the "rake 2" sector.

The effect of inlet Mach number on radial profiles of inlet velocity was negligible.

## Radial Profiles of Exit Velocity

The profiles of Fig. 4 represent plots, for three equally spaced circumferential positions, of the ratio of axial velocity at a radial position to average axial velocity in the diffuser exit plane. These profiles, which are typical for suction rates ranging from zero to about 10%, indicate that fully attached flow on both walls of the diffuser exit passage is not achieved. Instead the flow may be attached to the inner wall (hub biased profiles), or to the outer wall (tip biased profiles). It is particularly interesting to note that either type of bias can be obtained at identical inner and outer wall suction rates, depending on the order in which inner and outer wall suction is applied.

A typical illustration is shown in the figure for a suction condition given by $S_t = 6.2$ with $S_i = 2.5$ and $S_o = 3.7$. The hub biased profile of Fig. 4(a) was obtained by first applying suction on the inner wall, before outer wall suction was applied. When suction was momentarily interrupted on the inner wall ($S_i = 0$; $S_o = 3.7$) the profiles became tip biased. Suction was then reestablished on the inner wall ($S_i = 2.5$, $S_o = 3.7$). Instead of reverting to their original hub bias the profiles stayed tip biased as shown in Fig. 4(b), because, in effect, outer wall suction had been applied first. To reproduce the original hub biased profiles, the outer wall suction would have to be interrupted momentarily, which would have the same effect as applying inner wall suction first. Note that the circumferentially averaged inlet profile, shown for reference, remains unaltered.

Without suction ($S_t = 0$) the exit profiles were hub biased in about 90% of the cases. Momentary application of suction on the outer wall resulted in stable tip biased profiles, which could again be switched to hub biased by momentary application of inner wall suction.

The existence of either hub or tip bias at identical suction rates suggests that flat unbiased profiles are difficult to obtain over the entire annulus. The next three figures indicate this to be true. Figure 5 is a circumferential survey of the velocity ratio at radial positions equivalent to 10% (near hub) and 90% (near tip) of annular passage height. The total suction rate is 6.2% with $S_i = 2.5$ and $S_o = 3.7$. A nearly uniform hub bias is seen to exist over the annulus, as indicated by the high velocity ratio values for the 10% passage height and the low values for the 90% position. As the suction rate is increased to over 10% ($S_i = 4.0$, $S_o = 6.2$) (fig. 6(a)), the flow field becomes circumferentially segmented as revealed by the highly nonuniform circumferential distribution of velocity ratio values for the hub and tip radial positions. The figure shows sectors carrying flow with hub bias, tip bias, with unstable flow sectors in between. The unsteady flow is also illustrated by the irregular shape of the midspan velocity ratio plot shown in Fig. 6(b). At suction rates above 11% for diffuser A and about 15% for diffuser B unstable flow was observed over the entire annulus with individual flow sectors slowly undulating between hub and tip attachment.

The effect of inlet Mach number on radial profiles of exit velocity was negligible.

## Diffuser Effectiveness

This parameter, as defined by equation (3) expresses the ratio of actual to ideal conversic i of inlet dynamic pressure to exit static pressure. The effect of total suction rate, $S_t$ ($S_1/S_o \approx 0.7$), on diffuser effectiveness is shown in Fig. 7 for the two geometries tested. Although performance trends show a gross similarity, the improvement in diffuser effectiveness with suction rate follows a distinct curve for each diffuser. Diffuser A, starting at $\eta \approx 40\%$ at $S_t = 0$, achieves a peak effectiveness of about 87% at $S_t \approx 11$. Diffuser B, starting at $\eta \approx 47\%$ does not reach its peak effectiveness value of 85% until $S_t$ is increased to about 15. The performance of both diffusers deteriorates at suction rates above values at which $\eta$ is maximized. This is due to the onset of flow instability referred to previously.

Based on the results of Fig. 7, the performance improvement due to suction was greater for diffuser A than for diffuser B. The reason for this may be traced to the flow in the prediffuser exit plane which was attached to both walls in diffuser A but probably experienced local separation in the wider angle passage of diffuser B.

Diffuser effectiveness was found to be indepentent of inlet Mach number.

## Diffuser Total Pressure Loss

The total pressure loss curves for both diffusers (fig. 8) are consistent with the diffuser effectiveness trends. Pressure loss for diffuser A is seen to decrease more rapidly with suction, ranging from 1.2% at $S_t = 0$ to 0.4% at $S_t \cong 11$. The decrease is more gradual for diffuser B, namely from 1.1% at $S_t = 0$ to 0.5% at $S_t = 17$. Although the results plotted in Fig. 8 were obtained at $M_1 = 0.18$, the total pressure loss at other $M_1$ was found to correlate directly with $M_1^2$ at constant suction rate. Thus total pressure loss data obtained at low inlet Mach numbers could be extrapolated to inlet Mach numbers up to 0.41.

## CONCLUSIONS

Suction stabilized vortex flow diffusers show promise for application in combustors because of relatively high static pressure recovery and low total pressure loss obtained in a short length. Performance obtained using a narrow angle (7 degree) prediffuser was superior to that obtained with a prediffuser having a 14 degree included angle.

Symmetrical radial profiles of exit velocity were not obtained, since the diffuser exit flow showed preferential hub or tip attachment at moderate suction rates and became circumferentially nonuniform and unstable when a critical suction rate ($\approx 11\%$) was exceeded. This problem would be alleviated in a combustor application, since the combustor dome would cause some redistribution and stabilization of the flow.

A reversible profile bias effect was also noted at suction rates below 10%. In combustor applications this effect would make it possible to reverse the bias of the combustor inlet flow merely by momentary application of suction on the wall opposite the bias. Since suction would be only applied momentarily, the radial distribution of combustor airflow could be altered to meet requirements of particular operating conditions without penalizing engine cycle efficiency.

## REFERENCES

1. Ringleb, F. O., Flow Control by Generation of Standing Vortices and the Cusp Effect, Rep. 317, Princeton University, July 27, 1955.

2. Heskestad, G., Remarks on Snow Cornice Theory and Related Experiments with Sink Flows, J. Basic Eng., vol. 88, no. 2, June 1966, pp. 539-549.

3. Heskestad, G., Further Experiments with Suction at a Sudden Enlargement in a Pipe, ASME Paper 69-WA/FE-27, Nov. 1969; J. Basic Eng., vol. 92, no. 3, Sept. 1970, pp. 437-444.

4. Juhasz, Albert J., Performance of a Short Annular Dump Diffuser Using Wall Trailing Edge Suction, NASA TM X-3093, 1974.

5. Juhasz, Albert J., Effect of Wall Edge Suction on the Performance of a Short Annular Dump Diffuser with Exit Passage Flow Resistance, NASA TM X-3221, 1975.

6. Adkins, R. C., A Short Diffuser with Low Pressure Loss. Fluid Mechanics of Combustion, Proceedings of the Joint Fluids Engineering Conference, J. L. Dussourd, R. P. Lohmann, and E. M. Urim, eds., ASME, 1974, pp. 155-169.

7. Juhasz, Albert J. and Smith, John M., Performance of a High Area Ratio Annular Dump Diffuser Using Suction Stabilized Vortex Flow Control, NASA TM X-3535, 1977.

E-9011-1

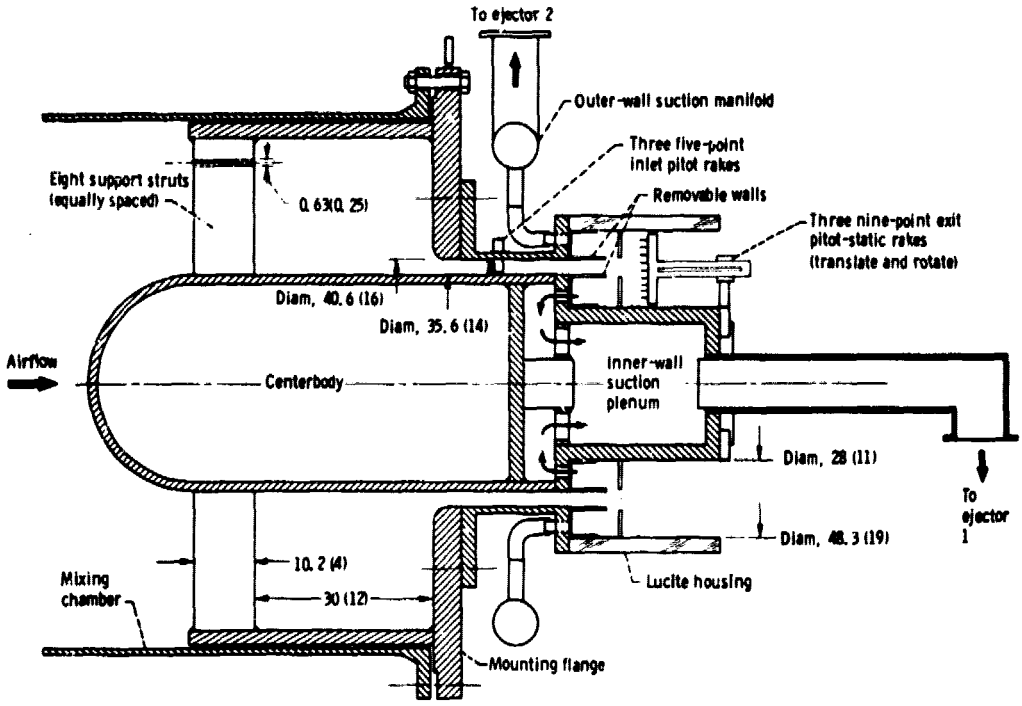


Figure 1. - Cross section of asymmetric annular diffuser test apparatus. (Dimensions are in cm (in.).)

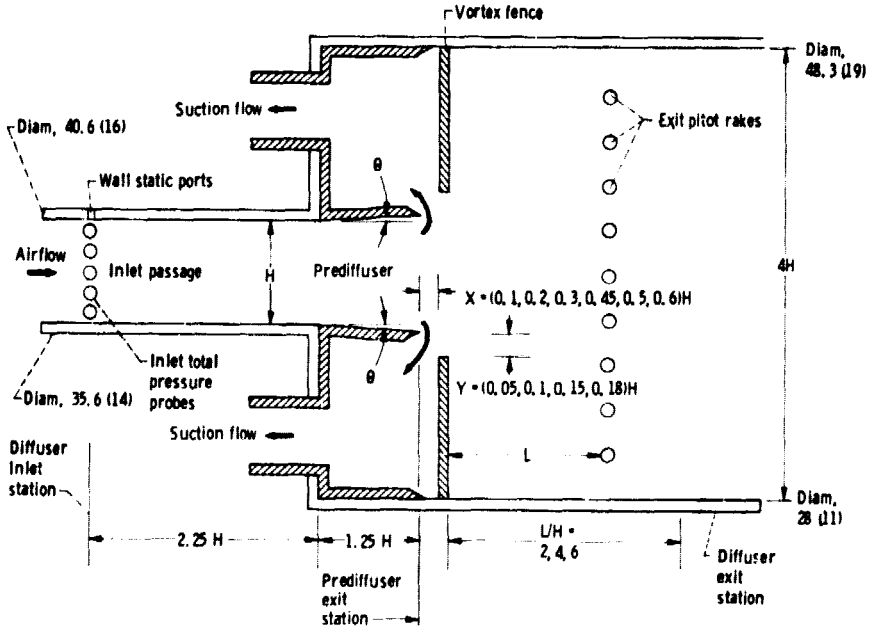


Figure 2. - Diffuser annulus passage details. Inlet passage height H = 2.54 cm (1.0 in.). (Dimensions are in cm (in.) unless otherwise indicated.)

ORIGINAL PAGE IS
OF POOR QUALITY

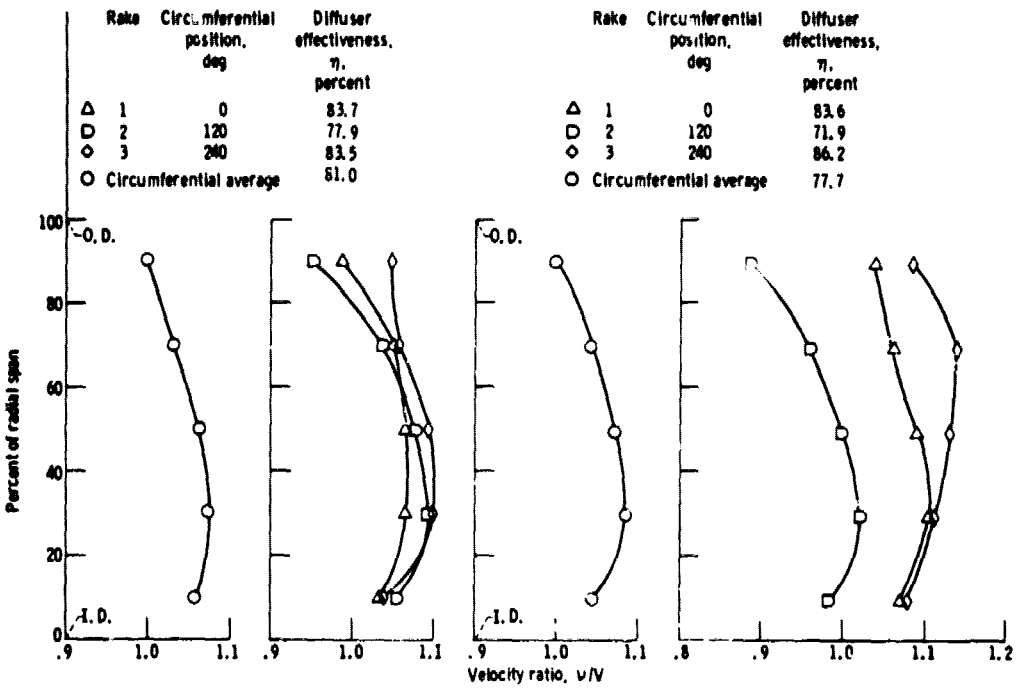


(a) Total suction rate $S_t$ = 9.9 percent.

(b) Total suction rate $S_t$ = 12.3 percent.

Figure 3. - Variation in radial profile of inlet velocity at three circumferential positions. Inlet Mach number $M_1$ = 0.18.

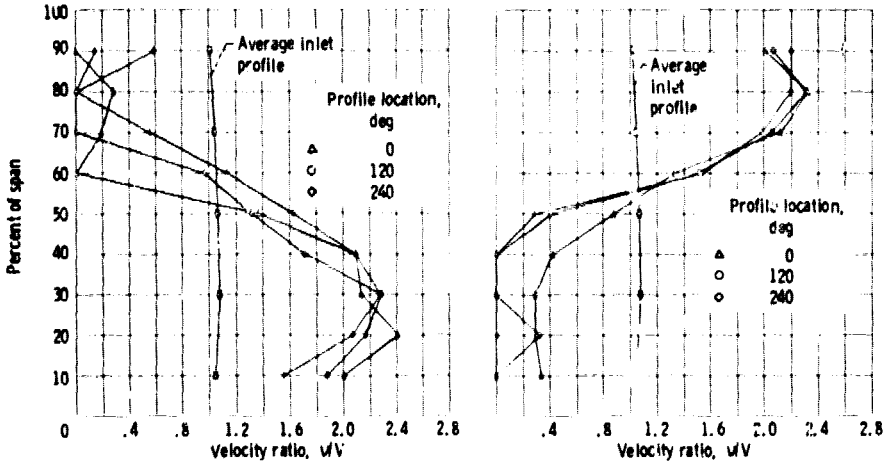


(a) Radial profiles of exit velocity at three circumferential locations showing hub bias by removing suction to outer wall vortex chamber momentarily and then reestablishing suction to outer wall prior to recording.

(b) Radial profiles of exit velocity at three circumferential locations showing tip bias by removing suction to inner wall vortex chamber momentarily and then reestablishing suction to inner wall prior to recording.

Figure 4. - Radial profiles of exit velocity at medium suction rates, illustrating bias reversal. Inlet Mach number, $M_1$ = 0.18, total suction rate $S_t$ = 6.2 percent.

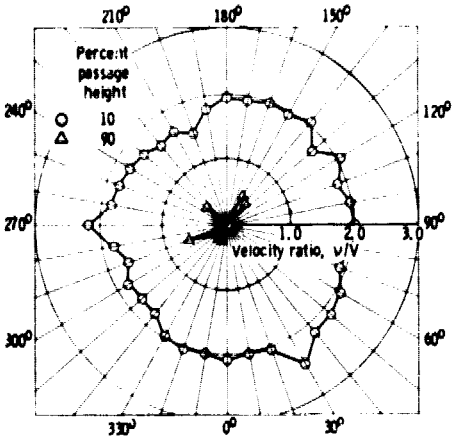


Figure 5. - Circumferential survey of exit velocity profiles at 10 and 90 percent of passage height at total suction rate of 6.2 percent. Inlet Mach number $M_1$ = 0.18; X = 0.45; Y = 0.15; exit rake position L/H, 6.0.

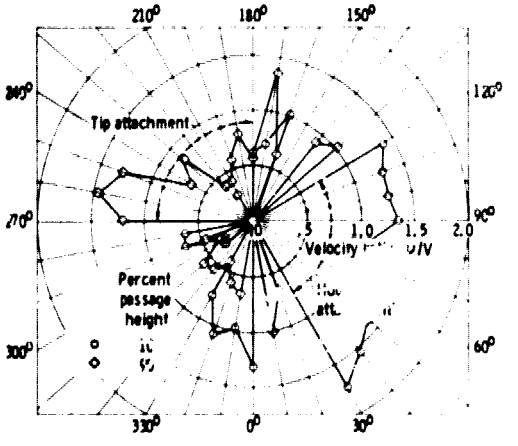


(a) Radial span position, 10 and 90 percent.

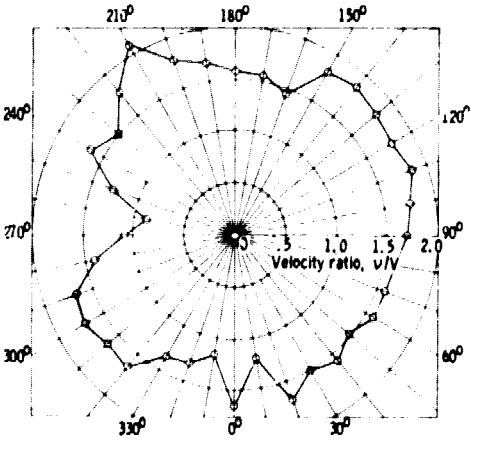


(b) Radial span position, 50 percent.

Figure 6. - Circumferential survey of velocity ratios at three radial span positions for a total suction rate of 10.2 percent. Inlet Mach number $M_1$ = 0.18; X = 0.45; Y = 0.15, exit rake position L/H = 6.0.

ORIGINAL PAGE IS
OF POOR QUALITY

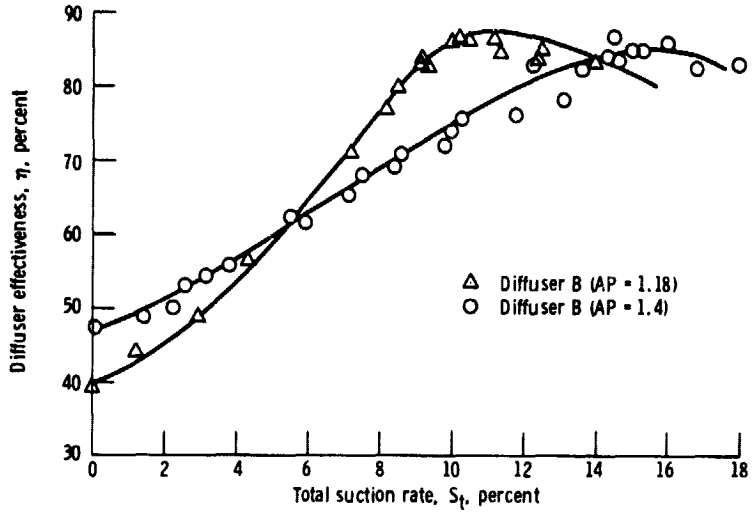


Figure 7. - Effect of suction on diffuser effectiveness.

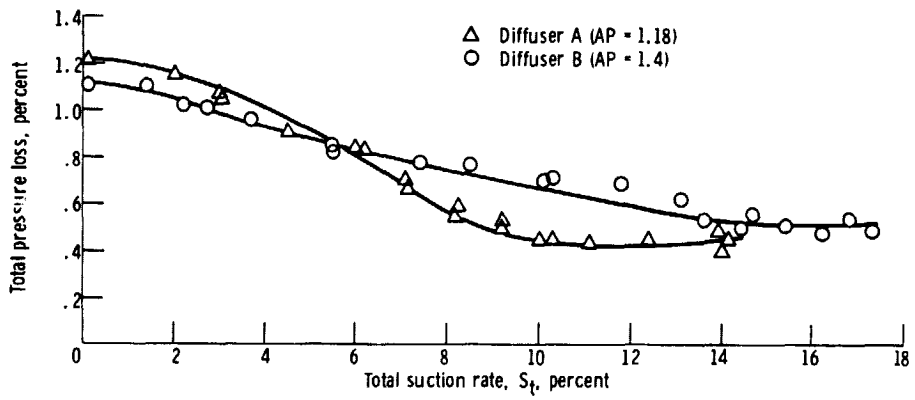


Figure 8. - Effect of suction on total pressure loss for $M_1 = 0.18$.